Journal of Sciences, Islamic Republic of Iran 23(3): 263-267 (2012) http://jsciences.ut.ac.ir
University of Tehran, ISSN 1016-1104

Electric-Field-Induced Triplet to Singlet Transition in Size-2 Trigonal Zigzag Graphene Nanoflake

M. Ghaffarian*

Department of Physics, Faculty of Science, University of Shahid Beheshti, Evin, Tehran, Islamic Republic of Iran

Received: 9 September 2012 / Revised: 22 September 2012 / Accepted: 9 October 2012

Abstract

Using Hartree-Fock Su-Sheriffer-Heeger (HF-SSH) model, we have studied the dependence of the energies of the ground (magnetic triplet state) and the first exited (nonmagnetic singlet state) states of the size-2 trigonal zigzag graphene nanoflake (size-2 NF) on the intensity of an external in plane static electric field at zero temperature. We identify a transition from the magnetic triplet state to a nonmagnetic singlet state in size-2 NF caused by the polarization energy induced by the in plane static electric field. This transition has a unique property of being accompanied by a sudden increase in the electric dipole moment of the size-2 NF.

Keywords: Graphene nanoflake; Hartree-Fock model; Transition; In-plane electric field

Introduction

In the past several years Graphene materials have emerged as promising materials for future electronic nanodevices [1-12]. In recent years new class of graphene derivatives known as nanodisks or nanoflakes have attracted much attention [13-25]. These two dimensional nanometer materials made of finite number of carbon atoms with closed edges have novel properties. Specially, the trigonal zigzag nanoflakes have been shown to posses edge states which in the noninteracting limit have zero energy and their number is equal to the size parameters, N, defined in Ref [26]. Further theoretical studies of the ground state of the low size parameter NF's have shown that the zero-energy states (edge states) determine the magnetic properties of NF and at half- filling the spins of electrons in the edge states due to the Coulomb exchange energy (Hund's rules) couple together ferromagnetically with large spin stiffness [26,27].

In this paper, based on the results obtained numerically, using HF-SSH model, we report on a transition in size-2 NF from the magnetic triplet state to a nonmagnetic[28] singlet state with sizable electric dipole moment, induced by externally applied in-plane static electric field at zero temperature. The justification for using the HF-SSH model is close similarity of the results of density function theory with the mean-field Hubbard model for low energy sector of nanoflakes [27].

The paper is organized as follows. In section II. We present the tight binding SSH model including the electron-electron interaction term in presence of in-plane external electric field. In the next section we present HF self consistent results for the total energies of the ground and first exited states and then by the effective Hamiltonan we consider the effect of in-plane static electric field on the two edge state of size-2 NF analytically which verify the numerical results. Section

* Corresponding author, Tel.: +98(912)7492603, Fax: +98(21)22431666, E-mail: m.ghaffarian@yahoo.com

IV is devoted to discution and conclusion.

Materials and Methods

The tight binding SSH Hamiltonian including the electron-electron Coulomb interaction for NF in the presence of an in-plane static electric field is

$$H = H_{SSH} + H_{int} + H_E \quad (1)$$

The first term is the SSH Hamiltonian[29] and has the following form

$$H_{SSH} = \sum_{<i,j>,\sigma} (-t - \alpha y_{ij}) c_{i\sigma}^{\dagger} c_{j\sigma} + \frac{K}{2} \sum_{<ij>} y_{ij}^2 \quad (2)$$

where i and j label the carbon sites of NF, <i,j> indicates summation over the nearest neighbors, $c_{i\sigma}^{\dagger}$ and $c_{j\sigma}$ are the creation and annihilation operators for fermions with spin σ , t is the hopping integral, α is the coupling constant between electron and phonon, y_{ij} is the change of the bond length between the *i*th and *j*th atoms which must be determined self consistently using the relation $y_{ij} = \sum_{\sigma} \frac{\alpha}{K} <c_{i\sigma}^{\dagger} c_{j\sigma}> - \frac{\alpha}{N_0 K} \sum_{<nm>,\sigma} <c_{n\sigma}^{\dagger} c_{m\sigma}>$ with N_0 equal to the number of carbon-carbon bonds, and finally K is the spring constant corresponding to carbon-carbon bond. The last term in Eq.(2) is the total energy due to change in the lengths of carbon-carbon bonds. We have used the following values for the aforementioned parameters of the SSH Hamiltonian: $t = 2.5eV$, $\alpha = 6.31 \frac{eV}{A^0}$ and $K = 49.7 \frac{eV}{A^{02}}$, taken from the Ref. [30,31].

The second term is the electron-electron Coulomb interaction where in the tight binding approximation is

$$H_{int} = U \sum_i (c_{i\uparrow}^{\dagger} c_{i\uparrow} - \frac{1}{2})(c_{i\downarrow}^{\dagger} c_{i\downarrow} - \frac{1}{2}) + \sum_{i \neq j} w\left(r_{i,j}\right) (\sum_{\sigma} c_{i\sigma}^{\dagger} c_{i\sigma} - 1) \times \left(\sum_{\tau} c_{i\tau}^{\dagger} c_{i\tau} - 1 \right) \quad (3)$$

where $r_{i,j}$ is the distance between the *i*th and *j*th carbon sites, and $w\left(r\right) = \frac{1}{\sqrt{\left(1/U\right)^2 + \left(r/r_0 V\right)^2}}$ is the Ohno potential[32]. The quantity U is the strength of onsite interaction, V is the strength of the long range part, and r_0 is the average distance of the carbon-carbon bond where for the graphene nanoflakes we have used the following values, respectively, $3.84eV$, $1.92eV$ and $1.42A^0$, taken from Ref. [27].

Finally, the last term is the coupling of the NF to the external in plane static electric field, **E**, given by

$$H_E = e\boldsymbol{E}.\sum_{i,\sigma} \boldsymbol{r}_i c_{i\sigma}^{\dagger} c_{i\sigma} + e\boldsymbol{E}.\sum_{<i,j>,\sigma} \tilde{\boldsymbol{r}}_{ij} c_{i,\sigma}^{\dagger} c_{j,\sigma} \quad (4)$$

where e is the charge of electron, $\boldsymbol{E}$ is the external static in plane electric field and $\mathbf{r}_i$ is the expectation value of the electron position operator, **r,** with respect to the Wannier state $|\varphi_i>$ which is equal to the carbon position, $\mathbf{r}_i = <\varphi_i|\boldsymbol{r}|\varphi_i>$. The second term in eq.(4) is the two-site terms describing the electric field assisted hopping of the electrons between neighboring carbon sites, where $\tilde{\boldsymbol{r}}_{ij} = <\varphi_i|\boldsymbol{r}|\varphi_j>$.

Results

1. Numerical Results

Taken the barycenter of NF as the origin and its top vertex on the y-axis the self-consistent HF solution of the total energies of the two low lying eigenstates as function of the external in plane static electric field intensity are numerically computed for various directions of the in plane electric field. Fig. 1 depicts our results on the total energies and energies due to the change in the carbon-carbon bonds for fully relaxed geometry of size-2 NF with the in plane electric field in the direction of y-axis. The contribution of the bond deformation energy to the total energies of the triplet and the singlet state are small compared to the electronic energies (see inset of the Fig. 2). At zero electric field the ground state due to Coulomb exchange energy is a spin triplet with total z-component of spin equal to one. The first excited state is a spin singlet with an energy gap of 0.595 eV with the ground state . As the intensity of the external electric field increases, due to the polarization energy, the energy gap between the ground state and the first exited state begins to diminish and for the electric field intensity greater than 0.164 Volt/a_0 the size-2 NF makes a transition to a spin singlet state which is the stable state and becomes nonmagnetic. To trace the effect of external in-plane static electric field on the spin and charge densities, we have plotted the self-consistent HF results of the total electric and magnetic dipole moments and the electric dipole moments of the core states of size-2 NF for the spin triplet and spin singlet states as functions of the field intensity in Figure 2. At the cross over from spin triplet state to spin singlet state the total magnetic moment vanishes and an increase of $\cong 4ea_0$ in the electric dipole moment of the size-2 NF occurs. This indicates that at the cross point to the spin singlet state the spin and charge densities of the spin triplet state are not stable and a sudden rearrangement of them in and between the two edge states of size-2 NF occurs. This rearrangement of spin and charge is, also, accompanied by changes in the length of carbon-carbon bonds which we show that causes reduction of the total electric dipole moment of the size-2 NF.

2. Effective Hamiltonian for Edge States

To get a deeper understanding of how the external static in-plane electric field initiates the transition from the spin triplet to spin singlet state and identifying the origin of the sizable increase in the total electric dipole moment of size-2 NF, following the arguments and the model proposed in Ref. [26] we consider the zero-energy sector (edge states) of size-2 NF which not only is determinant to the magnetic properties of the size-2 NF, we will show that its two basis vectors, also, have unique property of having sizable electric dipole moments with equal magnitudes but opposite directions.

The electronic Hamiltonian of the zero-energy sector for the size-N NF without the external in-plane electric field is

$$H_{eff} = \sum_{\alpha} U_{\alpha\alpha} n_{\uparrow}(\alpha) n_{\downarrow}(\alpha) + \frac{1}{2}\sum_{\alpha>\beta=1}^{N} U_{\alpha\beta} n(\alpha) n(\beta) - 2\sum_{\alpha>\beta=1}^{N} J_{\alpha\beta} \boldsymbol{S}(\alpha).\boldsymbol{S}(\beta) \quad (5)$$

where α and β label the zero-energy states, $U_{\alpha\beta}$ and $J_{\alpha\beta}$ are the direct and exchange parts of the Coulomb potential and $n(\alpha)$ and $\boldsymbol{S}(\alpha)$ are the second quantized density and spin operators of the zero-energy states given, respectively, by $n(\alpha) = \sum_{\sigma} c_{\sigma}^{\dagger}(\alpha) c_{\sigma}(\alpha)$ and $\boldsymbol{S}(\alpha) = \frac{1}{2}\sum_{\sigma',\sigma} c_{\sigma'}^{\dagger}(\alpha)\, \boldsymbol{\sigma}_{\sigma',\sigma}\, c_{\sigma}(\alpha)$ with $\boldsymbol{\sigma}$ designating the Pauli matrices ($\hbar = 1$).

The coupling of the edge states to the external in-plane static electric field adds the term $\sum_{\alpha,\beta=1}^{N}\sum_{\sigma}(\boldsymbol{E}\,\boldsymbol{d}_{\alpha\beta}) c_{\sigma}^{\dagger}(\alpha) c_{\sigma}(\beta)$ to the effective Hamiltonian, where $\boldsymbol{d}_{\alpha\beta}$ are the matrix elements of the dipole operator between the zero-energy states. For size-2 NF, we have listed their values in Table 1.

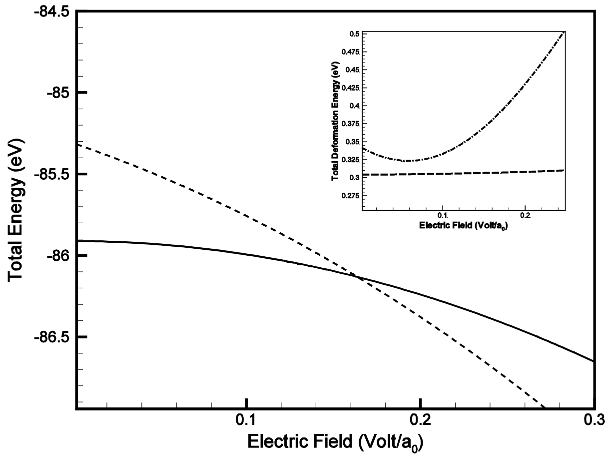

Figure 1. Total energies of the magnetic triplet state (solid line) and the first exited nonmagnetic singlet state (dashed line) of size-2 NF versus the intensity of external in plane static electric field, for the field in the y-direction. The inset presents the contribution of the carbon-carbon bounds deformation energies to the total energies of the ground state (dashed line) and the first exited state (dash-dotted line). At E=0.164 Volt/a_0 where a_0 is the Bohr radius, the size-2 NF makes a transition from the magnetic triplet state to a nonmagnetic singlet state.

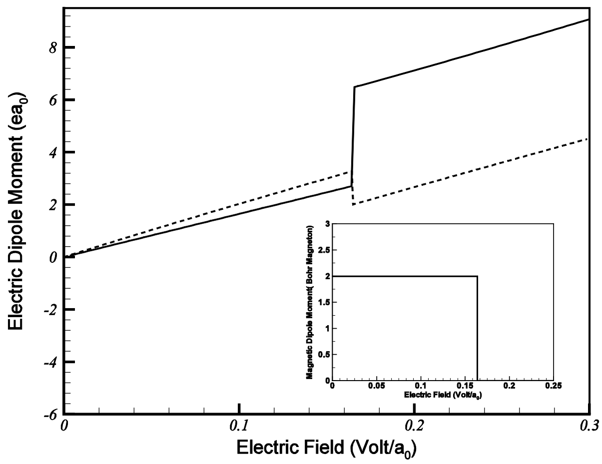

Figure 2. y-component of the total electric dipole moment (solid line) and the electric dipole moment of the core states (dashed line) of size-2 NF versus the intensity of the external in plane electric field, for the field in the y-direction. The inset represents the total magnetic dipole moments versus the intensity of the external electric field. Before the jump the size-2 NF is in the magnetic triplet state, after the jump the state becomes a nonmagnetic singlet state with large electric dipole moment in the y-direction. e is the charge of electron and a_0 is the Bohr radius.

The above effective Hamiltonian with the external in plane static electric field commutes with the operator of the total spin and for size-2 NF the eigenenergy states of the two-particle sector of its Hilbert space which form a six-dimensional vector space can be determined exactly. If we designate the spatial part of the two zero-energy states by ψ and ϕ, in terms of the total spin eigenstates (χ_t, χ_s) the two-particle sector has a spin triplet, $1/\sqrt{2}[\psi(1)\phi(2)-\psi(2)\phi(1)]\chi_t$, and three different spin singlet $\psi(1)\psi(2)\chi_s$, $1/\sqrt{2}[\psi(1)\phi(2)+\psi(2)\phi(1)]\chi_s$, $\phi(1)\phi(2)\chi_s$, basis which the triplet states with total z-components of spin -1,0,1 are already the eigenvectors of $H_{eff}+H_E$ with eigenenergies equal to $1/2U_{12}-J_{12}+e(\boldsymbol{E}\,\boldsymbol{d}_{11}+\boldsymbol{E}\,\boldsymbol{d}_{22})$, $1/2U_{11}+1/2U_{12}-J_{12}+e(\boldsymbol{E}\,\boldsymbol{d}_{11}+\boldsymbol{E}\,\boldsymbol{d}_{22})$, and $1/2U_{12}-J_{12}+e(\boldsymbol{E}\,\boldsymbol{d}_{11}+\boldsymbol{E}\,\boldsymbol{d}_{22})$. Since $\boldsymbol{d}_{11}=-\boldsymbol{d}_{22}$, the quantity $\boldsymbol{E}\,\boldsymbol{d}_{11}+\boldsymbol{E}\,\boldsymbol{d}_{22}$ is eqal to zero (see Table 1). This means that the external electric field dose not couple to the magnetic triplet state of size-2 NF directly, and the major part of polarization energy and electric dipole moment of the magnetic triplet state must be due to the core states. For the spin singlet states the situation is different. The external in plane electric field mixes the three spin singlet states and the effective Hamiltonian including the in plane electric field has the form

$$H_{eff}+H_E=\begin{pmatrix} U_{11}+2e\boldsymbol{E}\,\boldsymbol{d}_{11} & e\boldsymbol{E}\,\boldsymbol{d}_{12} & 0 \\ e\boldsymbol{E}\,\boldsymbol{d}_{21} & \frac{1}{2}U_{12}+3J_{12} & e\boldsymbol{E}\,\boldsymbol{d}_{12} \\ 0 & e\boldsymbol{E}\,\boldsymbol{d}_{21} & U_{22}+2e\boldsymbol{E}\,\boldsymbol{d}_{22} \end{pmatrix} \quad (6)$$

where $U_{11}=U_{22}=0.145U$, $U_{12}=0.0482U$ and $J_{12}=U_{12}$ Ref. [26]. For the static electric field in the direction of y-axis we can neglect the off diagonal elements since they depend on the y-components of $\boldsymbol{d}_{12}$ and $\boldsymbol{d}_{21}$ which are very small (see Table 1) The eigenenergies are then, $U_{11}+eE_y d_{11}^{(y)}$, $\frac{7}{2}U_{12}$ and $U_{11}-eE_y d_{11}^{(y)}$. We see that the energy of the spin singlet state constructed from the zero-energy state, ϕ, due to its negative dipole moment is decreasing function of the intensity of the in plane static electric field and for $|\boldsymbol{E}|>(\frac{7}{4})\frac{J_{12}}{ed_{11}^{(y)}}$ has lower energy than the triplet state. Thus, the major part of the electric dipole moment of the first exited state of the size-2 NF is due to the electric dipole moment of the edge state ϕ in the singlet state $\phi(1)\phi(2)\chi_s$, where the two electrons with opposite spin reside in it and the core states have minor contribution. The electric dipole moment due to the change in the length of carbon-carbon bonds can be determined by computing a negative derivative of the total deformation energy with respect to the intensity of the externa electric field. At transition point the resulting electric dipole moment is about 15 percent of the electronic electric dipole moment but with opposite direction. If we reverse the direction of the external in-plane electric field the energy of the singlet state, $\psi(1)\psi(2)\chi_s$, due to its positive dipole moment becomes decreasing function of the intensity of the in-plane static electric field and beyond the transition point size-2 NF acquires electric dipole moment opposite to the former case. This property is true for any direction of the external in-plane electric field. For $|\boldsymbol{E}|>\frac{1}{2e\,|\boldsymbol{d}_{11}|}\frac{1}{\sqrt{1+cos^2\theta}}[\frac{7}{2}+\frac{1}{2}cos^2\theta]J_{12}$ the size-2 NF makes a transition to nonmagnetic singlet state and acquires sizable electric dipole moment, due to its zero-energy states.

Furthermore, for $|\boldsymbol{E}|>(\frac{7}{4})\frac{J_{12}}{ed_{11}^{(y)}}$ the magnetic triplet state of the two-particle sector of the Hilbert space of the zero-energy sector is unstable and the magnetic triplet state with zero electric dipole moment makes a transition to the nonmagnetic singlet state, $\phi(1)\phi(2)\chi_s$, with sizable electric dipole moment.

Discussion

The above results support the HF-SSH finding on the behavior of the total energies of the ground and the first exited states of size-2 NF as functions of intensity of the external in-plane electric field. At the transition point from the magnetic triplet state to the nonmagnetic singlet state the jump in the total y-component of the electric dipole moment of size-2 NF, depicted in Figure 2, is therefore due to the electric dipole moment of the edge state, ϕ, of the singlet state $\phi(1)\phi(2)\chi_s$. For

Table 1. x and y components of the matrix elements of the dipole operator between the zero-energy states of size-2 NF ($\boldsymbol{d}_{11}$, $\boldsymbol{d}_{22}$, $\boldsymbol{d}_{12}=\boldsymbol{d}_{21}$) in Bohr radius

$\boldsymbol{d}_{11}=<\psi\|\boldsymbol{r}\|\psi>$	$\boldsymbol{d}_{11}=<\phi\|\boldsymbol{r}\|\phi>$	$\boldsymbol{d}_{11}=<\psi\|\boldsymbol{r}\|\phi>$
$d_{11}^{(x)}=+0.003$	$d_{22}^{(x)}=-0.003$	$d_{12}^{(x)}=-2.685$
$d_{11}^{(y)}=+2.685$	$d_{22}^{(y)}=-2.685$	$d_{12}^{(y)}=+0.003$

arbitrary irection of the applied external in-plane static electric field we have the same result, the two zero-energy states produce large energy dipole moment when the state of size-2 NF is the nonmagnetic singlet state.

In conclusion, we have identified a transition, induced by external in-plane static electric field, from magnetic triplet state of the size-2 NF to a nonmagnetic singlet state at zero temperature, due to the induced polarization energy of its two edge states. This magnetic to nonmagnetic transition is accompanied by a sizable increase of the electric dipole moment of size-2 NF, which mimics a magnetic dipole to electric dipole transition. This property is of potential value for future electronic nanodevices.

References

1. Novoselov K. S. et al. Electric Field Effect in Atomically Thin Carbon Films. *Science* **306**, 666 (2004).
2. Novoselov K. S. et al. Two- dimensional gas of massless Dirac in graphene. *Nature (Londan)* **438**, 197 (2005).
3. Zhang Y. et al. Experimental observation of the quantum Hall effect and Berry's phase in graphene. ***Nature** (Londan)* **438**, 201 (2005).
4. Nakada K., Fujita M., Dresselhaus G., and Dresselhaus M.S. Edge state in graphene ribbons: Nanometer size effect and edge shape dependence *Phys. Rev. B* **54**, 17954 (1996).
5. Wakabayashi K., Fujita M., Ajiki H., Sigrist M. Electronic and magnetic properties of nanographite ribbons. *Phys. Rev. B* **59**, 8271 (1999).
6. Son Y. W., Cohen M. L., Louie S. G. Energy Gaps in Graphene Nanoribbons. *Phys. Rev. Lett* **97**, 216803 (2006).
7. Han M. Y., Ozyilmaz B., Zhang Y., and Kim P. Energy Band-Gap Engineering of Graphene Nanoribbons *Phys.Rev. Lett* **98**, 206805 (2007).
8. Wang X., Ouyang Y., Li X., Wang H., Guo J., and Dai H. Room-Temperature All-Semiconducting Sub-10-nm Graphene Nanoribbon Field-Effect Transistors, *Phys. Rev. Lett* **100**, 206803 (2008).
9. Stampfer C., Guttinger J., Hellmuller S., Molitor F., Ensslin K., and Ihn T. Energy Gaps in Etched Graphene Nanoribbons. *Phys. Rev. Lett* **102**, 056403(2009).
10. Xu Z., Zheng Q., and Chen G. Elementary building blocks of graphene-nanoribbon-based electronic devices. *Appl .Phys .Lett* **90**, 223115(2007).
11. Yan Q. et al., Intrinsic Current−Voltage Characteristics of Graphene Nanoribbon Transistors and Effect of Edge Doping. *Nano. Lett* **7**, 1469 (2007).
12. Y. W. Son, M. L. Cohen, and S. G. Louie. Half-metallic graphene nanoribbons**.** *Nature* **444**,347 (2007).
13. Ezawa M. Metallic graphene nanodisks: Electronic and magnetic properties . *Phys. Rev. B* **76**, 245415 (2007).
14. Ezawa M. Quasiphase transition and many-spin Kondo effects in a graphene nanodisk. *Phys. Rev. B* **79**, 241407(R) (2009).
15. Berger C. et al. Electronic Confinement and Coherence in Patterned Epitaxial Graphene. *Science* **312**, 1191 (2006).
16. Rader H. J. et al. Processing of giant graphene molecules by soft-landing mass spectrometry . *Nat. Mater* 5, 276 (2006).
17. Wang W. L., Meng S., and Kaxiras E. Graphene NanoFlakes with Large spin. *Nano. Lett* **8**, 241 (2008).
18. Wang W. L., Yazyev O. V., Meng S., and Kaxiras E. Topological Frustration in Graphene Nanoflakes: Magnetic Order and Spin Logic Devices. *Phys. Rev. Lett.* **102**, 157201 (2009).
19. Akola J., Heiskanen H. P., and Manninen M. Edge-dependent selection rules in magic triangular graphene flakes. *Phys. Rev.B* **77**, 193410 (2008).
20. Yazyev O. V. Emergence of magnetism in graphene materials and nanostructures. *Rep. Prog. Phys* **73**, 056501 (2010).
21. Guclu A. D., Potasz P., Voznyy O., Korkusinski M., and Hawrylak P. Magnetism and Correlations in Fractionally Filled Degenerate Shells of Graphene Quantum Dots. *Phys. Rev. Lett* **103**, 246805 (2009).
22. Wurm J., Rycerz A., Adagideli I., Wimmer M., Richter K., and Baranger H. U. Symmetry Classes in Graphene Quantum Dots: Universal Spectral Statistics, Weak Localization, and Conductance Fluctuations. *Phys. Rev. Lett* **102**, 056806 (2009).
23. Potasz P., Guclu A. D., and Hawrylak P. Zero-energy states in triangular and trapezoidal graphene structures. *Phys. Rev. B* **81**, 033403 (2010).
24. Zhang Z. Z., Chang K., and Peeters F. M. Tuning of energy levels and optical properties of graphene quantum dots. *Phys. Rev. B* **77**, 235411 (2008).
25. Zhou J., Wang Q., Sun Q., and Jena P. Intrinsic ferromagnetism in two-dimensional carbon structures: Triangular graphene nanoflakes linked by carbon chains. *Phys. Rev. B* **84**, 081402(R) (2011).
26. Ezawa M. Coulomb blockade in graphene nanodisks. *Phys. Rev. B* **77**, 155411 (2008).
27. Fernandez-Rossier J., and Palacios J. J. Magnetism in Graphene Nanoislands. *Phys. Rev. Lett* **99**, 177204 (2007).
28. We determine the magnetic property of an state by computing the difference between the spin up and spin down densites at each carbon site of size-2 NF. For singlet state this quantity is zero at all the sites of size-2 NF.
29. Su W. P., Schrieffer J. R., and Heeger A. J. Soliton excitations in polyacetylene. *Phys. Rev. B* **22**, 2099 (1980).
30. Dong J., Jiang J., Yu J., Wang Z. D., and Xing D. Y. Nonlinear optical properties of the substituted fullerenes $C_{59}X$ (X=B,N). *Phys. Rev. B* **52**, 9066 (1995).
31. Harigaya K. Lattice distortion and energy-level structures in doped C_{60} and C_{70} molecules studied with the extended Su-Schrieffer-Heeger model: Polaron excitations and optical absorption. *Phys. Rev. B* **45**, 13676 (1992).
32. Ohno K. Some remarke on the Pariser-Parr-Pole method. *Theor. Chim. Acta* **2**, 219 (1964).